PHYSICAL REVIEW B, VOLUME 64, 161404(R)

Temperature dependence of the current-voltage characteristics of a carbon-nanotube heterojunction

Jinhee Kim,[1] Jeong-O Lee,[2] Hwangyou Oh,[2] Kyung-Hwa Yoo,[1] and Ju-Jin Kim[2]
[1]*Electronic Device Group, Korea Research Institute of Standards and Science, Yusong-gu, Taejon 305-600, Korea*
[2]*Department of Physics, Chonbuk National University, Chonju 561-756, Korea*
(Received 14 June 2001; published 3 October 2001)

Electrical transport properties of a heterojunction consisting of two multi-wall carbon nanotubes were studied. The current-voltage characteristics of the junction exhibited reproducible rectifying behavior which could be explained well by the Schottky barrier junction model in the intermediate temperature region. The barrier height and the diffusion potential were determined by fitting the current-voltage characteristics to the generalized diode equation. Noticeable deviations from the ideal behavior were observed both in high and low-temperature regions.

DOI: 10.1103/PhysRevB.64.161404 PACS number(s): 73.30.+y, 73.63.Fg, 73.40.Ei

Carbon nanotube (CNT) is a macro-scale molecule with noble electrical and mechanical properties.[1] CNTs can be either metallic or semiconducting depending upon their chirality, diameter, and length.[2–4] Since the discovery of CNTs there have been many efforts to use them for electronic devices. A variety of CNT-based electronic devices, such as single electron transistor,[5,6] field effect transistor,[7–9] cross junction,[10] and heterojunction[11–14] have been realized and studied. It has been shown that the low-dimensional nature of the electronic transport in CNT modifies the device characteristics significantly.[5,13,14] Theoretical studies on a CNT/CNT junction showed that the charge depletion region could extend over the entire tube due to the long-range Coulomb interaction in a single-wall CNT.[14] A heterojunction made of two different types of single-wall CNTs then was expected to give *I-V* characteristics different from that of conventional semiconductor heterojunction.[15]

In this paper we report the temperature dependence of the *I-V* characteristics of a CNT heterojunction consisting of two different types of multi-wall CNTs. Our major findings are (1) the multi-wall CNT heterojunction exhibits reproducible rectifying behavior and (2) the temperature dependence of the *I-V* characteristics is well explained by the conventional Schottky-barrier junction (SBJ) model in the intermediate temperature region and (3) the semiconducting multi-wall CNT in our sample is more like an intrinsic one than a heavily doped degenerated one.

The multi-wall CNTs synthesized by arc discharge method were prepared on a Si substrate with 500-nm-thick thermally grown SiO_2 layer. The patterns for electrical leads were generated by using electron beam lithography onto the selected CNT and then 20 nm of Ti and 50 nm of Au were deposited successively on the contact area by thermal evaporation. To form a stable Ohmic contact between the CNT and the Ti/Au electrode, we performed rapid thermal annealing at 600–800 °C for 30 s in vacuum.[16,17] Each metal/CNT contact exhibited a symmetric *I-V* characteristics in the whole measured temperature range and possible formation of a SBJ in the contact was excluded.

Figure 1 is the scanning electron micrograph of the sample which consists of two straight multi-wall CNTs connected in a kink with an angle of $\theta \approx 23°$. The kink was formed naturally during the sample growing process and the two straight CNTs, having almost an identical diameter of about 30 nm, were considered to be connected seamlessly with a heptagon-pentagon defect in the kink region.[11] Two CNTs connected seamlessly with a kink have different chiralities, which can be manifested by different energy gap. We measured the *I-V* characteristics of each straight CNT in the two-probe measurement configuration. As shown in Fig. 2(a), the upper CNT exhibited vanishing differential conductance at low bias voltages. The differential conductance increased almost linearly above the gap region. We took the energy gap by extrapolating the linear fitting curve in the high bias region to the voltage axis. Since there were two contact junctions connected in series, the energy gap was doubled. The energy gap of the upper CNT was then estimated to be about 150 meV. The lower CNT, on the other hand, exhibited a depleted but nonzero differential conductance at zero bias as shown in Fig. 2(b).[18]

Consisting of two straight CNTs which have different energy gaps, the sample can be considered as a heterojunction. The upper CNT is a semiconducting one with an energy gap of 150 meV and the lower CNT is either metallic or semiconducting. If the lower CNT is metallic, it is natural to consider the kink as a metal-semiconductor junction with probable formation of a SBJ.[19] If the lower CNT is a small gap semiconductor, the kink can be considered as an isotype heterojunction, consisting of two *p*-type semiconductors.[20]

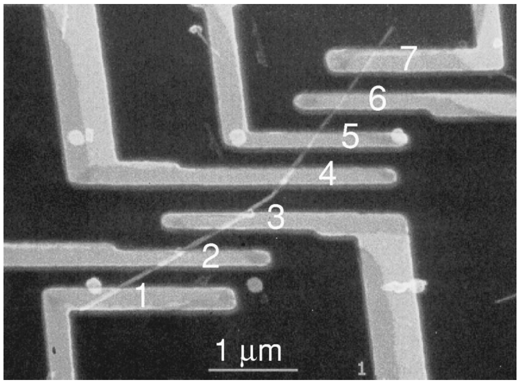

FIG. 1. The scanning electron microscope image of the sample. The kink junction is shown between the electrodes 3 and 4.

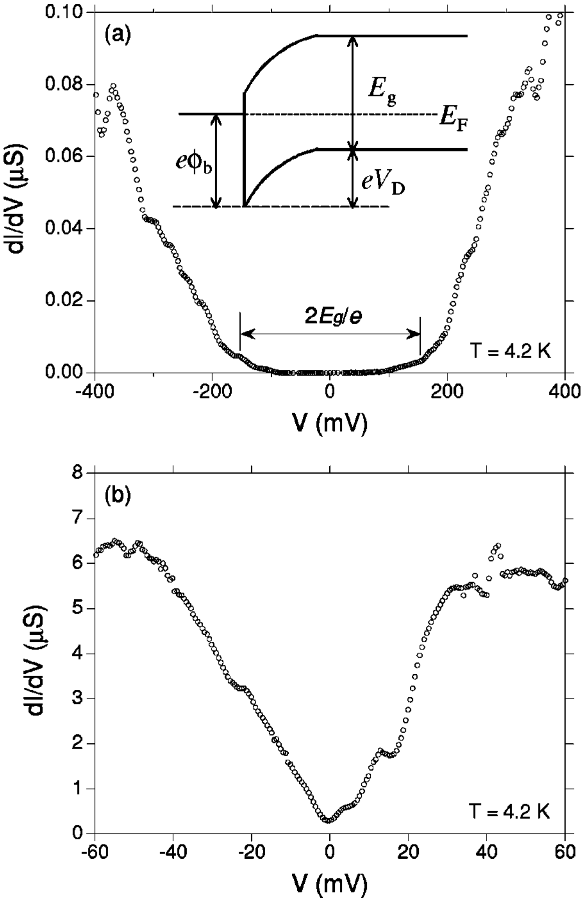

FIG. 2. Differential conductance-voltage (dI/dV-V) curves of (a)the upper CNT (electrodes 4 and 6) and (b) the lower CNT (electrodes 1 and 2) at temperature $T=4.2$ K. Shown in the inset of (a) is the schematics of the Schottky-barrier junction.

For a $p-p$ heterojunction, a spikelike bending is formed in the valence-band edge of the larger gap semiconductor.[15] If the energy gaps of the two semiconductors are widely different from each other, as in our case, the effect of the spikelike bending can be neglected and the SBJ is a good model system for the heterojunction. The inset of Fig. 1(b) shows the schematic energy band diagram of the SBJ. Determination of the barrier height (ϕ_b) and the diffusion potential (V_D) is essential in understanding the electrical transport properties of the SBJ.

We measured the I-V characteristics across the kink. Unlike those of the straight parts, the I-V characteristics of the kink was highly asymmetric and exhibited rectifying behavior as shown in the main panel of Fig. 3. Rectifying behavior was observed for any selection of electrodes across the kink and nonlinear behavior persisted up to 250 K. Both two- and four-probe measurements gave similar I-V characteristics. As shown in the inset in the upper left corner of Fig. 3, the current began to increase sharply at a certain voltage known as the threshold voltage, V_{th}, in the forward bias condition (a positive bias voltage applied to the upper CNT). At low temperatures V_{th} was nearly identical to the diffusion potential V_D (Ref. 19) and we thus obtained $V_D \approx 65$ mV. Another noticeable feature of the differential conductance curves at

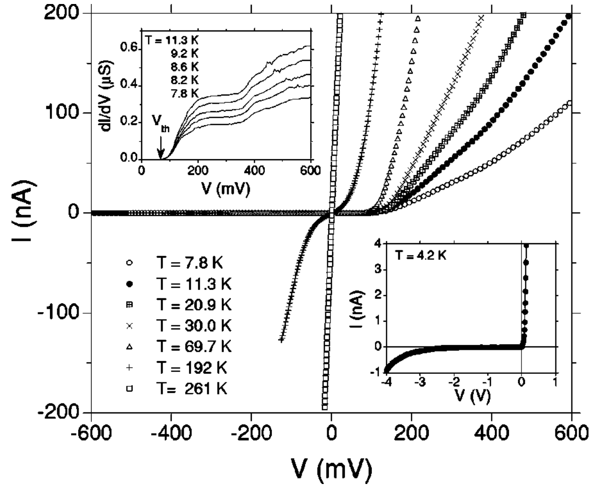

FIG. 3. I-V characteristics of the junction (electrodes 3 and 6) at temperatures listed in the figure. Inset in the upper-left corner shows the differential conductance-voltage curves of the junction at low temperatures. The overall view of the I-V characteristics at temperature $T=4.2$ K is shown in the inset in the lower-right corner.

low temperatures was the occurrence of constant conductance region at voltages $200 \text{ mV} < V < 300$ mV, which was attributed to the effect of the series resistance. The inset in the lower right corner of the Fig. 3 shows the wide range I-V curve at $T=4.2$ K. Note that the reverse bias breakdown occurs rather smoothly, in contrast to the sharp onset of the forward bias current.

A SBJ is said to be ideal if its I-V characteristics fits well to the diode equation

$$I=I_0\left[\exp\left(\frac{eV}{kT}\right)-1\right], \tag{1}$$

where I_0 is the reverse bias saturation current given by[19]

$$I_0=AT^2\exp\frac{-e(\phi_b-\Delta\phi_{bi})}{kT}. \tag{2}$$

Here A is the Richardson constant and $\Delta\phi_{bi}$ is the barrier change due to the bias voltage and the thermal fluctuation. If the image force lowering is the main cause of the barrier change, it can be shown that

$$\Delta\phi_{bi}=C\left(V_D-V-\frac{kT}{e}\right)^{1/4}, \tag{3}$$

where C is a constant dependent upon the dielectric constants and the impurity concentration. In general, the ideal behavior of a SBJ is rather exceptional. For many reasons, the I-V characteristics of real SBJ deviates from the ideal behavior. We fitted the I-V characteristics of the kink to the generalized diode equation,

$$I=I_0[\exp(\alpha V)-1]. \tag{4}$$

Here I_0 and α are fitting parameters. For an ideal SBJ, $\alpha = e/kT$ must be satisfied.

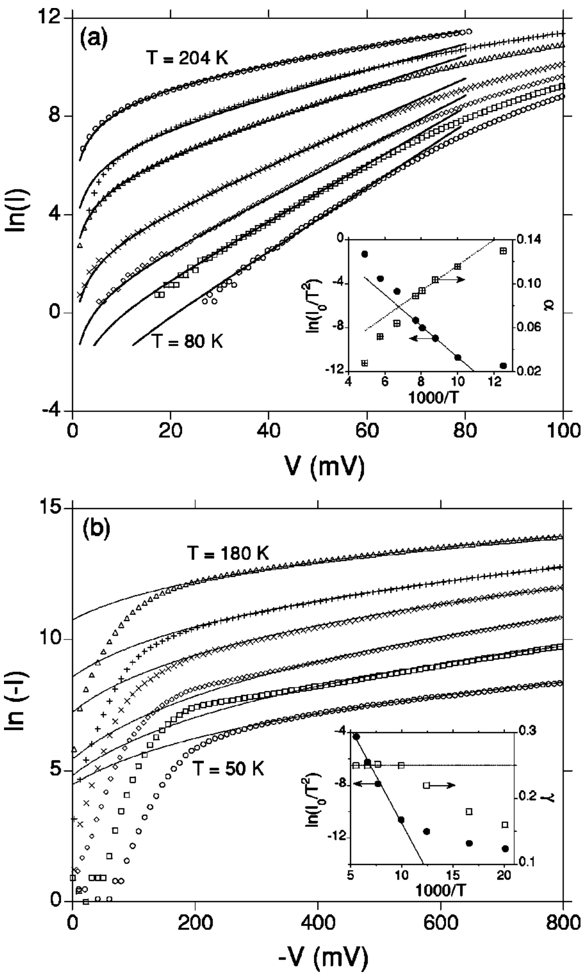

FIG. 4. (a)*I-V* characteristics of the junction in the forward bias condition (symbols) with the fitting curves (solid lines) at temperatures $T=80$, 100, 114, 130, 150, 174, 204 K. Inset shows the temperature dependence of the fitting parameters, I_0/T^2 (filled circle) and α (crossed square). (b) *I-V* characteristics of the junction in the reverse bias condition (symbols) with the fitting curves (solid lines) at temperatures $T=50$, 80, 100, 130, 150, 180 K. Inset shows the temperature dependence of the fitting parameters, I_0/T^2 (filled circle) and γ (empty square).

Shown in Fig. 4(a) are the semi-logarithmic plot of the *I-V* curves of the junction in the forward bias condition for several temperatures along with the best fitting curves to Eq. (4). In the temperature range $T=80$ K–204 K, the forward bias characteristics fits relatively well to the generalized diode equation in the low bias region. Noticeable deviation in the high bias region reveals that single transport mechanism may not explain the *I-V* characteristics in the whole bias range. The temperature dependence of the fitting parameters is shown in the inset of Fig. 4(a). The fitting parameter α satisfies the relation $\alpha=e/kT$ in the temperature range $T=100$ K–130 K. In this temperature range the reverse bias saturation current I_0 is expected to follow the temperature dependence given in Eq. (2). Since the image force lowering can be neglected in the forward bias condition, the linear slope of $\ln(I_0/T^2)$ vs $1/T$ gives the barrier height ϕ_b. We obtained the barrier height $\phi_b=124.2$ mV.

We also fitted the *I-V* characteristics in the reverse bias condition to the generalized diode equation. For a sufficiently large reverse bias voltage, Eqs. (1)–(3) give

$$\ln(-I)\approx\ln(I_{r0})+\frac{C(V_D-V)^{1/4}}{kT}, \tag{5}$$

where $I_{r0}=AT^2\exp(-e\phi_b/kT)$. For a convenience, we also take the exponent 1/4 as a fitting parameter γ

$$\ln(-I)=\ln(I_0)+\frac{C(V_D-V)^{\gamma}}{kT}. \tag{6}$$

Figure 4(b) shows the reverse bias characteristic of the junction with the best fitting curves to the above equation. In the temperature range $T=50$ K–200 K, the reverse bias characteristics of the sample was fitted well to the above equation in the high bias region. The diffusion potentials obtained by fitting were in the range $V_D=55$ mV–70 mV and exhibited a weak temperature dependence. Note that the diffusion potential obtained from the reverse bias characteristics was nearly identical to the diffusion potential estimated from the threshold voltage in the forward bias condition, 65 mV. Shown in the inset of Fig. 4(b) are the fitting parameters γ and $\ln(I_0/T^2)$ as a function of temperature. Note that γ was close to the expected value 1/4 in the temperature range $T=100$ K–200 K but exhibited a noticeable deviation from 1/4 at temperatures below 80 K. By linear fitting of $\ln(I_0/T^2)$ to $1/T$ in the temperature range $T=100$ K–200 K, we obtained the barrier height $\phi_b=123.9$ mV. The barrier height obtained from the reverse bias characteristics was almost identical to that obtained from the forward bias characteristics.

The *I-V* characteristics of the kink junction exhibited noticeable deviation from the ideal behavior both in low- and high-temperature regions. In particular, α exhibited saturated behavior at low temperatures (see the inset of Fig. 5). The saturated behavior of α in the low temperature region is well known for the conventional semiconductor SBJ and is generally attributed to the quantum tunneling effect.[19] The tunneling effect is non-negligible for the SBJ with a heavily doped semiconductor. For our sample, however, the semiconducting CNT is very lightly doped. The Fermi level of the semiconducting CNT (upper one) lies deep inside the energy gap, i.e., 59 meV above the valence-band edge and 91 meV below the conduction-band edge. The semiconducting CNT is more like an intrinsic one than a heavily doped one. Our observations then suggest that a simple tunneling model may not explain the saturated behavior of α at low temperatures. We have found that the fitting of α to the conventional tunneling model gives a poor result. Such discrepancy may be attributed to the effect of interlayer tunneling between neighboring graphene sheets. Note also that the effect of defect or deformation in the CNT may not be neglected at low temperatures.

Nonideal behavior of the *I-V* characteristics was also observed at high temperatures. With the increase of the temperature, in addition to the thermionic emission, other transport mechanisms also begin to contribute to the total current. Among several known transport mechanisms, the electron-hole recombination current and the effect of the series resis-

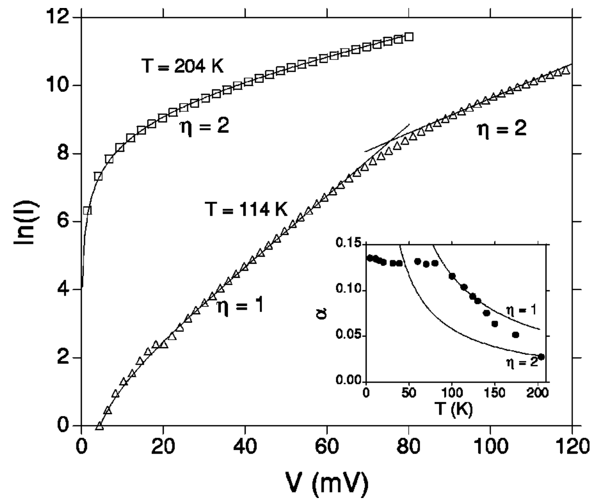

FIG. 5. *I-V* characteristics of the junction in the forward bias condition at temperatures $T=114$ K (empty triangle) and 204 K (empty square). The solid lines are fitting curves to the generalized diode equation with $\eta=1$ in the low bias region and $\eta=2$ in the high bias region at $T=114$ K and $\eta=2$ in the whole range at $T=204$ K. Inset shows the temperature dependence of the fitting parameter α obtained from the *I-V* characteristics in the forward bias condition along with the constant-η curves, $\eta=eV/\alpha kT=1$ and 2.

tance are worth mentioning. If the recombination current is a dominant transport mechanism, α is given by $\alpha=e/2kT$. If we define $\eta=e/\alpha kT$, $\eta=1$ corresponds to the thermionic emission current and $\eta=2$ to the recombination current. A smooth transition from $\eta=1$ to $\eta=2$ occurs if one increases either bias voltage or temperature. For our sample, η was in the range $1<\eta<2$ (see the inset of Fig. 5) in the temperature range $T=50$ K–220 K. As shown in Fig. 5, the transition from $\eta=1$ to $\eta=2$ with the increase of the bias voltage is evident at the temperature $T=114$ K. On the other hand, the *I-V* characteristics at temperature $T=204$ K is well fitted to $\eta=2$ in the whole bias range. Such behavior was also observed in a conventional semiconductor SBJ.[19] With the further increase of the bias voltage, in addition to the recombination current, the effect of the series resistance becomes non-negligible, giving linear *I-V* characteristics or constant differential conductance curve as shown in the inset of Fig. 3.

Due to the long-range Coulomb interaction in the low-dimensional system, the electronic transport properties of a CNT SBJ are believed to be different than from those of the conventional semiconductor SBJ.[13,14] Previous studies have shown that the single-wall CNT SBJs have reverse bias breakdown voltages comparable in magnitude to the forward bias threshold voltage.[11,13] For our sample, however, the reverse bias breakdown voltage, -2 V, was far greater in magnitude than the forward bias threshold voltage, 65 mV. Furthermore, theory predicted that the depletion length of a single-wall CNT SBJ changed sensitively on the doping concentration, giving the depletion length comparable to or greater than the entire tube length for a lightly doped CNT.[14] Such a long depletion length means that usual rectifying behavior may not be observed in a lightly doped CNT SBJ. For our sample, however, clear rectifying behavior was observed although the semiconducting CNT was considered to be very lightly doped. These observations suggest that the long-range Coulomb interaction assumed for the single-wall CNT may not apply to the multi-wall CNT. Due to their larger diameter, multi-wall CNTs are expected to have better electrostatic screening and shorter screening length than single-wall CNTs. Short screening length of multi-wall CNT SBJ can explain why the *I-V* characteristics of multi-wall CNT SBJ is closer to that of conventional semiconductor SBJ than that of single-wall CNT SBJ.

This work was supported by Korea Research Foundation Grant (KRF-2001-015-DP0179). This work was also supported by the Electron Spin Science Center at POSTECH, Korea.

[1] C. Dekker, Phys. Today **52**(5), 22 (1999).
[2] M.S. Dresselhaus, G. Dresselhaus, and P.C. Eklund, *Science of Fullerenes and Carbon Nanotubes* (Academic, New York, 1996).
[3] J.W.G. Wildöer *et al.*, Nature (London) **391**, 59 (1998).
[4] T.W. Odom, J.-L. Huang, P. Kim, and C.M. Lieber, Nature (London) **391**, 62 (1998).
[5] M. Bockrath *et al.*, Science **275**, 1922 (1997).
[6] S.J. Tans *et al.*, Nature (London) **386**, 474 (1997).
[7] S.J. Tans, A.R.M. Verschueren, and C. Dekker, Nature (London) **393**, 49 (1998).
[8] R. Martel *et al.*, Appl. Phys. Lett. **73**, 2447 (1998).
[9] K. Liu, M. Burghard, S. Roth, and P. Bernier, Appl. Phys. Lett. **75**, 2494 (1999).
[10] M.S. Fuhrer *et al.*, Science **288**, 494 (2000).
[11] Z. Yao, H.W.Ch. Postma, L. Balents, and C. Dekker, Nature (London) **402**, 273 (1999).
[12] C. Papadopoulos *et al.*, Phys. Rev. Lett. **85**, 3476 (2000).
[13] A.A. Odintsov, Phys. Rev. Lett. **85**, 150 (2000).
[14] F. Léonard and J. Tersoff, Phys. Rev. Lett. **85**, 4767 (2000).
[15] A.G. Milnet and D.L. Feucht, *Heterojunctions and Metal-Semiconductor Junctions* (Academic Press, New York, 1972).
[16] Y. Zhang *et al.*, Science **285**, 1719 (1999).
[17] J.-O Lee *et al.*, J. Phys. D **33**, 1953 (2000).
[18] If we assume that the lower CNT is an armchair nanotube, the upper CNT has chirality index (m,n) which has a relation with the junction angle θ as follows, $\cos\theta=\sqrt{3}(m+n)/2\sqrt{m^2+n^2+mn}$.
[19] E.H. Rhoderick and R.H. Williams, *Metal-Semiconductor Contacts* (Clarendon Press, Oxford, 1988).
[20] Though we have not shown here, two straight CNTs exhibited weak *p*-type gating effect, consistent with previous experimental results by other groups.